Research Article

Received: 3 February 2023 Revised: 25 April 2023 Accepted article published: 17 May 2023 Published online in Wiley Online Library: 1 June 2023

(wileyonlinelibrary.com) DOI 10.1002/jsfa.12706

Application of near-infrared spectroscopy for the estimation of volatile compounds in Tempranillo Blanco grape berries during ripening

Sandra Marín-San Román,[a] Juan Fernández-Novales,[b,c*] Cristina Cebrián-Tarancón,[d] Rosario Sánchez-Gómez,[d] María Paz Diago[b,c*] and Teresa Garde-Cerdán[a*]

Abstract

BACKGROUND: The knowledge of volatile compounds concentration in grape berries is very valuable information for the wine-maker, since these compounds are strongly involved in the final wine quality, and in consumer acceptance. In addition, it would allow to set the harvest date according to aromatic maturity, to classify grape berries according to their quality and to make wines with different characteristics, among other implications. However, so far, there are no tools that allow the volatile composition to be measured directly on intact berries, either in the vineyard or in the winery.

RESULTS: In this work, the use of near-infrared (NIR) spectroscopy to estimate the aromatic composition and total soluble solids (TSS) of Tempranillo Blanco grape berries during ripening was evaluated. For this purpose, the spectra in the NIR range (1100–2100 nm) of 240 intact berry samples were acquired in the laboratory. From these same samples, the concentration of volatile compounds was analyzed by thin film-solid-phase microextraction-gas chromatography–mass spectrometry (TF-SPME-GC–MS), and the TSS were quantified by refractometry. These two methods were used as reference methods for model building. Calibration, cross-validation and prediction models were built from spectral data using partial least squares (PLS). Determination coefficients of cross-validation (R^2_{CV}) above 0.5 were obtained for all volatile compounds, their families, and TSS.

CONCLUSIONS: These findings support that NIR spectroscopy can be successfully use to estimate the aromatic composition as well as the TSS of intact Tempranillo Blanco berries in a non-destructive, fast, and contactless form, allowing simultaneous determination of technological and aromatic maturities.

Keywords: aromatic composition; NIR spectroscopy; non-destructive; partial least squares; TF-SPME; total soluble solids (TSS)

INTRODUCTION

Grape and wine quality and value are directly related to the aromatic compounds that come from the berries, also called varietal aroma.[1-3] Therefore, the study of these compounds is highly relevant, since it is related to the acceptance or rejection of the wine by the consumer.[4] The aromatic characterization of Spanish white varieties has been little studied,[5] particularly that of *Vitis vinifera* L. Tempranillo Blanco.[6-8] This variety is a natural mutation of *Vitis vinifera* L. Tempranillo, and has been grown since 2008 only in the Appellation d'Origine Contrôlée (A.O.C.) Rioja. Today, *Vitis vinifera* L. Tempranillo Blanco is the second white variety (12%) grown in the A.O.C. Rioja in terms of surface area, after *Vitis vinifera* L. Macabeo (a. k. a. Viura) (70%).[6,7,9] The fact that it is an exclusive variety of the A.O.C. Rioja gives it a special value to the producing area and allows it to be differentiated from other regions.

* *Correspondence to: J Fernández-Novales or M Paz Diago, Departamento de Agricultura y Alimentación, Universidad de La Rioja, Madre de Dios 53, Logroño, 26007, Spain, E-mail: juan.fernandezn@unirioja.es; maria-paz.diago@unirioja.es and T Garde-Cerdán, Grupo VIENAP, Instituto de Ciencias de la Vid y del Vino (CSIC, Universidad de La Rioja, Gobierno de La Rioja), Ctra. de Burgos, Km. 6, 26007 Logroño, Spain. E-mail: teresa.garde.cerdan@csic.es*

a *Grupo VIENAP, Instituto de Ciencias de la Vid y del Vino (CSIC, Universidad de La Rioja, Gobierno de La Rioja), Logroño, Spain*

b *Grupo TELEVITIS, Instituto de Ciencias de la Vid y del Vino (Universidad de La Rioja, CSIC, Gobierno de La Rioja), Logroño, Spain*

c *Departamento de Agricultura y Alimentación, Universidad de La Rioja, Logroño, Spain*

d *Cátedra de Química Agrícola, E.T.S. de Ingeniería Agronómica y de Montes y Biotecnología, Departamento de Ciencia y Tecnología Agroforestal y Genética, Universidad de Castilla-La Mancha, Albacete, Spain*

The volatile compounds present in grape berries are found in very low concentrations (ng/L to mg/L),[10] therefore, it is necessary to conduct a previous sample preparation step before chromatographic analysis.[3,11]

Analytical techniques, such as gas chromatography–mass spectrometry (GC–MS), have numerous drawbacks, including time consumption, sample preparation, reagent and instrumentation costs, the need for trained personnel among others.[3] Moreover, they are destructive. All these reasons prevent the winemaker from measuring the volatile compounds in the grapes throughout the ripening period. However, a good understanding and knowledge of the concentration of these compounds in the berries would enable the winemaker to make decisions regarding viticultural practices, the date of harvest, or to classify and grade the fruit according to its aromatic quality, hence to separate in different fermentation tanks according to their characteristics and final price.[12,13] This has become even more important in recent years due to the imbalance between industrial maturity (whose main measurement parameter is the total soluble solids, TSS) and phenolic and aromatic maturities, caused by global warming and climate change.[14] As a result, berries reach the appropriate TSS content (°Brix), which is the most used parameter used by winemakers to schedule the harvest date, but the proper content of phenolic and aromatic compounds is not always achieved.[15,16] In order to solve these problems, fast and non-destructive methods have been developed to relate multivariate spectroscopic and chemical data to the concentration of specific chemical components associated with grape quality.[17-19]

One of these technologies is near-infrared (NIR) spectroscopy which is a very powerful tool for non-invasive measurement of quality parameters during the grape ripening.[12,18,20-24] NIR spectroscopy is based on the relationship between the physico-chemical property to be measured and the absorption of light at different wavelengths in the NIR region (750–2500 nm).[18,23,25,26] This technique is under constant evolution, in terms of instrumentation, as well as the mathematical algorithms used to extract and process the information provided by the spectral data (chemometric analysis).[25,27] Some of the main advantages of NIR spectroscopy include rapid data collection, non-destructive measurement of samples, low cost, and accurate measurement.[21,23,27-32] Some studies focused on NIR spectroscopy to measure different quality parameters in grape berries and wines have been published in the last decade. Among them, some works have focused on the estimation of general parameters (pH, tartaric acid, density, malic acid, gluconic acid, assimilable nitrogen, etc.),[19,22,26,33,34] TSS,[12,21,30,35] amino acids,[12] phenolic compounds,[20,26,36-38] or acids.[35]

Regarding the content of volatile compounds, there are some works that have studied the wine aromatic composition[13,29,39-42] using NIR spectroscopy, but only a very limited number of them have focused on grape berries.[18,43-45] Therefore, the aim of this work was to evaluate the efficacy of NIR technology to assess the evolution of the aromatic composition and TSS of *Vitis vinifera* L. Tempranillo Blanco grape berries along ripening, during two vintages.

MATERIALS AND METHODS

Vineyard characteristics and experimental design

The *Vitis vinifera* L. Tempranillo Blanco clusters were collected during the 2019 and 2020 seasons in a vineyard owned by the Gobierno de La Rioja, located in Finca La Grajera (Logroño, La Rioja, Spain). The clusters were hand-picked randomly. The exact location of the vineyard plot is: 42°26'26.23″ north latitude 2° 30'51.25″ west latitude; 447 m above sea level. The grapevines were grafted onto 110 Richter rootstock and were trained to a vertically shoot positioned system. The vineyard was planted in 2002 in an east–west orientation, and with a spacing between rows and within the row of 3.00 m × 1.10 m, respectively. Samples were collected from veraison to postharvest in both seasons. In 2019 clusters were collected along five dates: 12 August 2019, 19 August 2019, 26 August 2019, 2 September 2019, and 9 September 2019. In 2020 clusters were collected along seven dates: 29 July 2020, 5 August 2020, 12 August 2020, 19 August 2020, 26 August 2020, 2 September 2020, and 9 September 2020. At each date, 25 plastic bags were filled with 2–3 clusters of Tempranillo Blanco in each one. The clusters were frozen at −20°C until sample preparation.

Sample preparation

All frozen bunches belonging to the same collected date were manually destemmed in a tray. The berries were mixed manually until homogenization was achieved. Finally, 20 bags were labeled and prepared, and 64 berries from the tray were added to each bag. The same process was repeated for all dates, until 20 bags, with 64 berries, were obtained per date. At the end of the process, 100 samples were obtained (5 dates × 20 samples/date) for 2019, and 140 samples (7 dates × 20 samples/date) for 2020, giving a total of 240 samples between the two seasons.

NIR spectroscopy measurements

Spectral data were acquired using a NIR spectrometer operating in the range of 1100–2100 nm (PSS 2120, Polytec GmbH, Waldbronn, Germany) under laboratory conditions (Fig. 1). This spectrometer has a 2 nm resolution, with 501 datapoints per spectrum.[12] The spectrometer includes a polychromator as reflection light source selector, and an indium gallium arsenide (InGaAs) diode array detector. This device presents a sensor head (based on an integrated 20 W tungsten halogen lamp) for light capturing, a processing unit and an optical fiber linking them. Each spectrum was recorded under laboratory conditions at room temperature (23 °C) in reflectance mode by an average of 32 scans, without any sample preparation (directly on intact grape berries). The height between the sensor head and the sample to be acquired was 250 mm. The sensor head is provided with an embedded white and dark reference mechanism triggered by the software. As advised by the spectrometer's manufacturer, white and dark reference measurements were performed at the

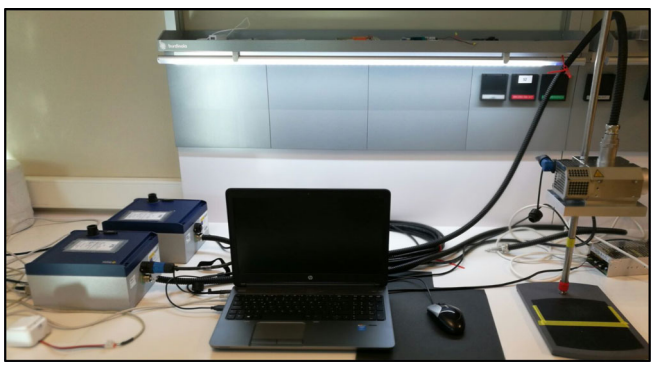

Figure 1. NIR spectrometer covering the range 1100–2100 nm.

Journal of The Science of Food and Agriculture published by John Wiley & Sons Ltd on behalf of Society of Chemical Industry.

beginning of the day and every 200 spectra approximately. The white reference material is referred to as a Spectralon™-like material by the manufacturer. Spectra were corrected using the white and dark reference values according to Eqn (1).

$$R(\lambda)=\frac{G(\lambda)-D(\lambda)}{W(\lambda)-D(\lambda)} \quad (1)$$

where λ is a wavelength (in nanometers), G is the intensity of the light reflected by the berries (in nanometers), W is the intensity of the light coming from the white reference (in nanometers), and D is the dark reference (in nanometers). Afterwards, the reflectance (R) was converted into absorbance [log(1/R)] (in nanometers).

For the spectral contactless measurement of the 240 samples, eight subsamples consisting of eight berries each were measured and averaged. In this way, the 64 berries that formed each sample were measured (eight subsamples × eight berries). These berries were placed on a plate (fruit holder) within the measurement area, with the pedicel of berries downwards to avoid differences between the berry surface and the pedicel (Fig. 2(a)). Between samples, the plate was cleaned to remove previous residues. Berry samples were naturally thawed at ambient temperature, and they were carefully dried with kimwipe paper before their measurement with NIR.

Analysis of TSS and volatile compounds

Materials and reagents

Chromatographic standards α-terpineol, geraniol, linalool, β-damascenone, β-ionone, benzaldehyde, 2-phenylethanol, benzyl alcohol, octanoic acid, decanoic acid, 2-hexenal, hexanal, 1-hexanol, 2-hexen-1-ol, 2-octanol (internal standard, IS), and the reagent sodium chloride (NaCl) and ethanol (EtOH), were purchased from Merck (Darmstadt, Germany). Water was purified through a Milli-Q system (Millipore, Bedford, MA, USA).

Thin film (TF) with polydimethylsiloxane and carboxen (PDMS/CAR) (carbon fabric film thickness 450 µm), liners packed with Tenax TA™, and borosilicate magnetic stirrers were obtained from GERSTEL GmbH & Co (Mülheim an der Ruhr, Germany). BP21 capillary column [30 m length, 0.25 mm inner diameter (i.d.), and 0.25 µm film thickness] was purchased from SGE (Ringwood, Australia).

Blender was bought from Philips (Amsterdam, the Netherlands). The refractometer, oven, and six-position stirrer plates were purchased from Actylab (Logroño, La Rioja, Spain). Gas chromatograph (Agilent 7890A) and mass spectrometer (Agilent 5975C) were purchased from Agilent Technologies (Palo Alto, CA, USA). The autosampler system consisted of a multi-purpose sampler (MPS) equipped with 98 tube tray, thermal desorption unit (TDU), and cooled injection system (CIS-4) connected to a cryostatic cooling device (CCD2). MPS, automated TDU, and CCD2 were provided from GERSTEL.

TSS measurement by refractometry

The same 64 berries from which the NIR spectra was acquired, were triturated for 30 s in the blender. The paste obtained was introduced into a 50 mL Falcon, and centrifuged at 3900 rpm, for 15 min. For each sample, TSS were measured with a refractometer, adding a few drops of the centrifuged must, and expressed as °Brix.

Extraction of volatile compounds by TF-SPME

For the volatile compound analysis, the extraction method of Marín-San Román *et al.*[46] was optimized. A 9 mL aliquot of centrifuged must sample were added in a 10 mL screw capped vial. In addition, 25 µL of the 2-octanol solution (5 µL 2-octanol/100 mL ethanol), and 2.5 g of NaCl, were added to the same vial. TF (PDMS/CAR) was suspended in the screw capped vial. All samples were stirred at 500 rpm, with a borosilicate magnetic stirrer, for 6 h at room temperature. After this time, the TF was removed with tweezers, dried with a tissue paper, and placed in a TDU tube with glass wool at the base. The TDU tube was sealed with a transport adapter and placed in a 98 position Twister rack on the MPS robotic for automated analysis. The analysis of volatiles was carried out on a GC–MS, equipped with an automated TDU.

Gas chromatography–mass spectrometry (GC–MS) conditions

The chromatographic method described in Sánchez-Gómez *et al.*[47] was used with some modifications adapted to the thin film-solid-phase microextraction (TF-SPME). TF-SPME devices were thermally desorbed at a constant pressure of 20.75 psi in the TDU, in splitless desorption mode, increasing the temperature from 40 °C to 250 °C at a rate of 60 °C/min and holding at the final temperature for 5 min. The analytes were focused in a

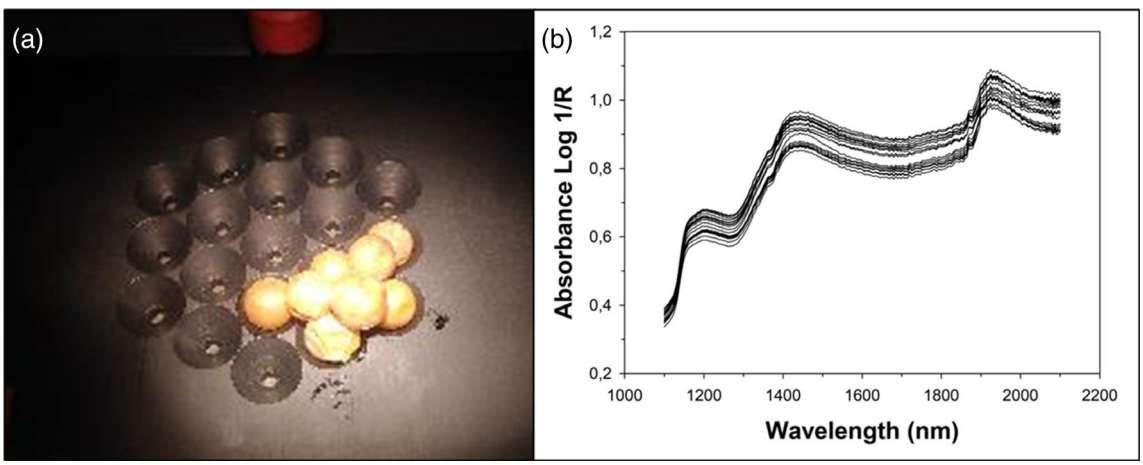

Figure 2. (a) Detail of the sensor during spectral acquisition on eight grapes berries with the NIR spectrometer, (b) average absorbance spectra of the 20 grape berry samples, forming date 1 (29 July 2020) of the 2020 vintage, in the NIR range.

programmed temperature vaporizing injector (CIS-4), containing a Tenax TA™ – packed liner with 20 mg of Tenax, held at −40 °C with the CCD2 prior to injection. After desorption and focusing, the CIS-4 temperature was programmed from −40 °C to 230 °C at 12 °C/s and held at 230 °C for 5 min to transfer volatiles onto the analytical column. The CIS-4 operated in solvent vent mode (purge flow to split vent of 80 mL/min at 2 min, vent 60 mL/min and pressure 20.85 psi). The desorbed volatile compounds were separated in the gas chromatograph system coupled to a quadrupole electron ionization mass spectrometric detector, equipped with a fused silica capillary column (BP21 stationary phase, 30 m length, 0.25 mm i.d. and 0.25 μm film thickness). The helium carrier gas had a constant column pressure of 20.75 psi. The oven temperature of GC was programmed at 40 °C (2 min), raised to 80 °C (5 °C/min, held for 2 min) then to 130 °C (10 °C/min, held 5 min) then to 150 °C (5 °C/min, held for 5 min) and finally to 230 °C (10 °C/min, held 5 min). Transfer line temperature was 235 °C. The MS operated in scan mode (35–180 amu) with ionization energy set at 70 eV. In order to identify each compound within the chromatogram, the mass spectra obtained were compared with those provided in the NIST library and with the retention time obtained for each standard. Compounds for which no standard was available were identified using the NIST library. All compounds were integrated in extraction ion chromatogram (EIC) mode by isolating the target ion of each compound individually. In this way, matrix interferences were eliminated. The target ions were *m/z* 41 for 2-hexenal, *m/z* 43 for acetic acid, *m/z* 45 for 2-octanol (IS), *m/z* 56 for hexanal, and 1-hexanol, *m/z* 57 for (*E*)-2-hexen-1-ol, and 2-ethyl-1-hexanol, *m/z* 59 for α-terpineol, *m/z* 60 for hexanoic acid, octanoic acid, nonanoic acid, and decanoic acid, *m/z* 67 for 3-hexen-1-ol, *m/z* 69 for citral, β-damascenone, and geraniol, *m/z* 71 for linalool, *m/z* 77 for benzaldehyde, *m/z* 79 for benzyl alcohol, *m/z* 91 for 2-phenylethanol, *m/z* 119 for *p*-cymene, and *m/z* 177 for β-ionone. Quantification was based on the calibration curves of the respective standards.

Calibration curves

The solutions of the calibration curves were analyzed by the method optimized by Marín-San Román *et al.*[46] TF-SPME under 500 rpm stirring, for 6 h, at 20 °C. Standard solutions were prepared in 50 mL of ethanol. Each one had different concentrations of each of the compounds. After extraction, they were desorbed and analyzed in GC–MS, performing three replicates of each. The compounds used, and the determination coefficients (R^2) of the calibration curves were the following: α-terpineol (0.9942), geraniol (0.9154), linalool (0.9643), β-damascenone (0.9684), β-ionone (0.9803), benzaldehyde (0.9684), 2-phenylethanol (0.9853), benzyl alcohol (0.9961), octanoic acid (0.9707), decanoic acid (0.9846), 2-hexenal (0.9937), hexanal (0.9898), 1-hexanol (0.9706), and 2-hexen-1-ol (0.9748). The curve of each compound is formed by a minimum of four points and a maximum of seven points of different concentrations. The concentration of some volatile compounds, for which no calibration curve was available, was then calculated using the calibration curve of another compound belonging to the same family, and whose concentration was in a similar range. Likewise, for citral, the linalool curve was used; for *p*-cymene, the α-terpineol curve was employed; for acetic, hexanoic, and nonanoic acids, the decanoic acid curve was utilized; and for 3-hexen-1-ol, the 2-hexen-1-ol curve was used.

Spectral data analysis

The spectral data collected with the Polytec PSS 2120 sensor were analyzed through the SL Utilities software (version 3.1; Polytec GmbH, Waldbronn, Germany). A visual analysis to examine the behavior of each subsample and detect possible anomalous spectra was carried out. The average spectrum of each sample was represented by averaging the eight spectra acquired of the eight subsamples, that is of the 64 berries.

The WinISI II software package version 1.50 (Infrasoft International, PortMatilda, PA, USA) was used for spectral data processing and statistical analysis of NIR spectra. For each analytical parameter, different mathematical treatments were evaluated for scatter correction, including the standard normal variate (SNV) and Detrending (DT) methods. Furthermore, two derivate mathematical treatments were tested in the development of NIR spectral calibrations models, in the spectral region 1600–2400 nm, where the first digit is the number of the derivative (*a*), the second is the gap over which the derivative is calculated (*b*), the third is the number of data points in a running average or smoothing (*c*), and the fourth is the second smoothing (*d*).[48] The averaged spectrum for each sample (Fig. 2(b)) was processed as input for a principal component analysis (PCA) in order to explore the data structure, to visualize the presence of spectra outliers and also to identify the main sources of variability in the spectra.[49,50] Modified partial least squares (MPLS) regression was used for the prediction of the individual and families of the volatile compounds and TSS using the spectra acquired on intact grape berries in the NIR range (1100–2100 nm). MPLS finds the combinations of predictor values that have the greatest covariance with the response.[51] To prevent over-fitting, the appraisal of the calibration model was performed by a four-fold cross-validation. In this method, the set of calibration samples was divided into four groups, using one of them to check the results (prediction) and the remaining (four groups) to build the calibration model. This was repeated as many times as groups were (four in total), in such a way that all the samples were used in both the calibration and prediction sets. In this process another type of outlier (chemical outliers) was analyzed using Student's *t* statistic, which indicates the difference between the reference and the predicted value. The Studentized residuals from the regression models fitted using least-squares is a very common approach to identifying discordant observations in linear regression problems.[52] A critical limit of $t > 2.5$ was used to identify samples as chemical outliers.[48] In order to train robust models, capable of predicting totally unknown samples, the original dataset, with 240 samples was split into two independent datasets: a calibration one, consisting of 192 samples (80%) assigned randomly, and a prediction set (20%), which comprised the remaining 48 samples (Table 1). Each set included samples that were appropriately distributed and covered the entire range of the volatile compounds and TSS. Although the same number of samples were used for the data set (240), for the calibration set (192), and for the external prediction set (48), not all the compounds could be found in all of them, so the *N* value may change in each of them (Table 1). The accuracy of the calibration depends on the model errors, patently, standard error of cross-validation (SECV) and standard error of prediction (SEP) used for internal validation or external prediction, respectively. The number of latent variables (LVs) and determination coefficients of calibration, cross-validation or external prediction (R^2_c, R^2_{cv} and R^2_p, respectively) to represent the proportion of explained variance of the response variables were also computed. The optimal number of LVs was selected as the one yielding the lowest SECV. Additionally, the

Journal of The Science of Food and Agriculture published by John Wiley & Sons Ltd on behalf of Society of Chemical Industry.

Table 1. Descriptive statistics of 20 volatile compounds content (μg/L), the total of each family content (μg/L), and total soluble solids (°Brix) of Tempranillo Blanco grape berries

	Data set					Calibration set					External prediction set				
Compounds	*N*	Minimum	Maximum	Mean	SD	*N*	Minimum	Maximum	Mean	SD	*N*	Minimum	Maximum	Mean	SD
Terpenoids															
α-Terpineol	236	0.022	5.41	0.69	1.14	189	0.022	5.41	0.68	1.15	47	0.024	3.24	0.77	1.11
Citral	233	1.24	301.19	34.11	52.43	186	1.24	301.19	34.05	53.91	47	3.25	180.09	34.33	46.64
Geraniol	172	0.12	76.85	2.38	6.89	132	0.12	76.85	2.64	7.77	40	0.27	9.58	1.54	2.10
Linalool	227	0.33	29.08	3.12	4.50	182	0.33	29.08	3.00	4.54	45	0.47	18.65	3.58	4.34
p-Cymene	238	0.032	17.92	0.97	2.32	191	0.032	17.92	0.98	2.45	47	0.038	7.36	0.92	1.69
Total terpenoids	238	0.69	333.74	39.74	58.23	191	0.69	333.74	39.49	59.78	47	4.46	204.47	40.75	52.06
C_{13} norisoprenoids															
β-Damascenone	234	0.00065	9.63	0.58	1.29	187	0.0006	9.63	0.53	1.25	47	0.00093	6.63	0.79	1.42
β-Ionone	238	0.0013	0.59	0.043	0.081	191	0.0013	0.59	0.04	0.08	47	0.0017	0.35	0.047	0.074
Total C_{13} norisoprenoids	238	0.0026	10.22	0.61	1.35	191	0.0026	10.22	0.56	1.31	47	0.0030	6.98	0.83	1.49
Benzenoids															
Benzaldehyde	235	0.14	10.29	1.67	1.86	188	0.14	10.29	1.66	1.88	47	0.21	6.79	1.73	1.78
2-Phenylethanol	238	7.07	330.70	60.20	73.53	191	7.07	330.70	60.00	75.05	47	12.50	318.89	61.02	67.76
Benzyl alcohol	237	1.30	90.35	11.64	14.52	190	1.30	90.35	11.36	14.40	47	2.50	77.52	12.77	15.08
Total benzenoids	238	9.09	401.78	73.44	88.91	191	9.09	393.11	72.93	90.30	47	15.50	401.78	75.52	83.97
Fatty acids															
Acetic acid	238	1.05	221.49	19.17	21.82	191	1.05	221.49	19.75	23.39	47	2.17	76.41	16.83	13.65
Hexanoic acid	238	0.59	153.97	10.15	19.69	191	0.59	153.97	10.46	20.17	47	0.77	96.68	8.88	17.76
Octanoic acid	238	0.18	17.59	1.85	2.44	191	0.18	17.59	1.90	2.60	47	0.19	6.95	1.66	1.68
Nonanoic acid	238	0.053	5.82	0.47	0.61	191	0.053	5.82	0.47	0.64	47	0.076	2.08	0.46	0.47
Decanoic acid	176	0.025	3.56	0.15	0.33	144	0.025	3.56	0.16	0.36	32	0.029	0.58	0.12	0.13
Total fatty acids	238	1.91	308.92	31.64	38.40	191	1.91	308.92	32.58	40.13	47	4.77	164.49	27.83	30.45
C6 compounds															
2-Hexenal	238	19.11	2137.39	270.69	364.00	191	19.11	2137.39	271.22	371.33	47	26.73	1369.71	268.56	336.30
Hexanal	238	10.17	3693.21	378.80	586.28	191	10.17	3693.21	379.87	608.50	47	14.56	2930.11	374.46	491.46
1-Hexanol	238	18.25	882.20	141.93	108.78	191	18.25	882.20	138.54	107.42	47	28.26	640.62	155.69	114.28
2-Hexen-1-ol	184	23.95	7964.66	1026.07	1207.08	147	23.95	7964.66	973.43	1192.02	37	27.07	5029.11	1235.18	1260.07
3-Hexen-1-ol	237	38.77	7680.73	903.07	1092.15	191	38.77	7680.73	875.39	1054.58	46	78.96	6455.88	1018.01	1242.24
Total C6 compounds	238	344.05	14 881.10	2483.96	2381.48	191	344.05	14 881.10	2414.20	2341.02	47	543.15	11 236.81	2767.43	2545.92
Total positive compounds	238	17.53	784.05	145.44	154.04	191	17.53	784.05	145.57	158.05	47	30.25	557.91	144.93	138.13
TSS	240	11.30	24.90	19.46	3.34	192	11.30	24.90	19.31	3.39	48	12.20	24.50	20.05	3.11

Note: *N*, number of samples; SD, standard deviation; TSS, total soluble solids; Total positive compounds, the sum of all families except C6 compounds.

J Sci Food Agric 2023; **103**: 6317–6329
Journal of The Science of Food and Agriculture published by John Wiley & Sons Ltd on behalf of Society of Chemical Industry.

wileyonlinelibrary.com/jsfa

residual predictive deviation (RPD_{CV}), calculated as the ratio between the standard deviation of the reference data for the training set and the SECV, together with the bias and slope, was also computed (Table 2).

RESULTS AND DISCUSSION

Content of grape volatile compounds and TSS

Table 1 shows the number of samples (*N*), mean, maximum and minimum value, and standard deviation of the 20 volatile compounds identified, their total content by chemical families, and TSS. The number of samples is different for each compound. This is due to the fact that, although the number of samples analyzed was 240, not all the compounds appeared in all chromatograms.

The volatile compounds were classified into six groups: terpenoids, C_{13} norisoprenoids, benzenoids, fatty acids, C6 compounds and total positive compounds (the total of all groups except C6 compounds).

Volatile compounds and TSS were measured from veraison to postharvest, covering a wide range of concentrations and ° Brix, as shown in Table 1. Volatile compounds concentration ranged from 0.0006 μg/L for β-damascenone to 7964.66 μg/L for 2-hexen-1-ol.

Terpenoids are the most studied varietal compounds in grapes and, in general, they are alcohols and oxides of ten carbon atoms.[53,54] They are synthesized during grape ripening, and are located mainly in the grape skin,[53] and are responsible for fruity and floral aromas.[55,56] They are found in berries in free and glycosylated form, being the glycosylated fraction the most abundant. In this work, five terpenoids were found (Table 1); α-terpineol, citral, geraniol, linalool, and *p*-cymene. α-Terpineol, geraniol, and linalool are some of the most odoriferous ones.[55] The most abundant terpenoid in Tempranillo Blanco was citral, followed by linalool (Table 1).

The C_{13} norisoprenoids are compounds derived from the enzymatic degradation of carotenoids.[57,58] Since C_{13} norisoprenoids are terpenes, they can also be found in grapes in free or bound form (glycoside glycosides). The C_{13} norisoprenoids are present in grape berries in very low concentrations, but they have a very low perception threshold (700 ng/L for β-ionone and 200 ng/L for β-damascenone), and therefore contribute significantly to the aromatic potential.[55] A positive correlation has been observed between C_{13} norisoprenoids and fruity aromas, especially in β-damascenone (apple juice and tropical fruit).[54] β-Ionone is related to violet aroma.[54] In *Vitis vinifera* L. Tempanillo Blanco, β-damascenone was the most abundant C_{13} norisoprenoid (Table 1). This result coincides with the only two works found in the literature that have studied the volatile composition of *Vitis vinifera* L. Tempranillo Blanco berries.[9,59]

Terpenoids and C_{13} norisoprenoids are two of the families that most contribute to the grape varietal aroma.[53,55]

Benzenoids are a diverse group of volatile compounds that can contribute significantly to the wine aroma.[60] They are synthesized late in the development of the grape, are present in very low quantities in grapes, and are mostly found as glycosylated precursors.[55,59] It can be observed that 2-phenylethanol, with a rose aroma descriptor,[61] was the most abundant benzenoid in *Vitis vinifera* L. Tempranillo Blanco musts, followed by benzyl alcohol, and finally benzaldehyde. These results are consistent with those obtained by García *et al.*[62] for grapes of the white varieties Airén, Macabeo (Viura), and Chardonnay. However, this result is not consistent with the results obtained in Gutiérrez-Gamboa *et al.*[59] and in Garde-Cerdán *et al.*[9] in *Vitis vinifera* L. Tempranillo Blanco grapes, where 2-phenylethanol was the least abundant benzenoid.

Fatty acids can be short chain (< 6 carbons), medium chain (6–12 carbons) and long chain (> 12 carbons).[60] In this work, five fatty acids were found, one of short chain (acetic acid), which was the most abundant, and is formed as a metabolic intermediate in the synthesis of acetyl-CoA,[60] and four corresponding to the medium chain group (hexanoic acid, octanoic acid, nonanoic acid, and decanoic acid).

The C6 compounds, also known as 'green leaf volatiles', are present in all grapes in free form.[53] These compounds are formed from fatty acids by the lipoxygenase pathway, and are responsible for the green aroma in the must.[60] The most abundant family of volatile compounds found in the *Vitis vinifera* L. Tempranillo Blanco berries was the C6 compound-family (Table 1). This result is consistent with the majority of studies on volatile compounds in red,[63-65] and white grape berries,[5,62] and specifically, also in *Vitis vinifera* L. Tempranillo Blanco berries.[9,59] The most abundant C6 compound was 2-hexen-1-ol (Table 1). Despite being very abundant compounds in grapes, they have a very high perception threshold, so they are among the least odorous compounds[53,54] having a more limited impact in final olfactory perception of the resulting wines.

With respect to the TSS, the range was from 11.30 °Brix, obtained in less ripe grapes, to 24.90 °Brix, corresponding to ripe grapes.

It can be observed that the standard deviation of the compounds was very high, this is due to the difference between the ripening stages of the grapes. Owing to carrying out such a wide and representative sampling allowed us to build robust models.

Analysis of NIR spectra

Figure 2(b) shows the average absorbance spectra of the 20 samples from the first sampling date of 2020, in the range 1100 to 2100 nm. Three absorption peaks can be identified. The first one, over 1143 nm, is assigned to the second C–H stretch overtone (aromatic structure and CH_3). The other two peaks, over 1450 nm and 1900 nm are respectively related to the first overtone of the symmetric and asymmetric hydroxyl (O–H) bond stretching and the combination of stretch and deformation of this group in water, which is the predominant constituent of grape berries.[12,23]

Calibration, cross-validation, and external prediction results for the NIR models of volatile compounds content and TSS

Table 2 shows the mathematical pre-treatments that provided the best results in calibration, cross-validation, and external prediction for each volatile compound, their families, and the TSS. As in Table 1, the standard deviation of the volatile compounds was higher than the mean, because the berries were harvested at different ripening times in order to obtain a wide range of both volatile compounds and TSS.

Different mathematical treatments were tested in the development of NIR spectral calibrations set (*a*, *b*, *c*, *d*), as previously discussed. In Table 2, *N* corresponds to the number of samples in the calibration set, excluding the chemical anomalies (eliminating the samples that had $t > 2.5$). Table 2 also shows the values of R^2_C, R^2_{CV}, and R^2_P, which correspond to the coefficient of determination of the calibration, cross-validation, and prediction, respectively. Volatile compounds, families and TSS with R^2_{CV} values

Journal of The Science of Food and Agriculture published by John Wiley & Sons Ltd on behalf of Society of Chemical Industry.

Table 2. Calibration, cross-validation, and external prediction results for the near-infrared (NIR) models of volatile compounds content (μg/L), the total of each family content (μg/L), and total soluble solids (°Brix) in Tempranillo Blanco grape berries

						Calibration		Cross-validation			External prediction			
Compounds	Spectral treatment	*N*	Mean	SD	LV	SEC	R^2_C	SECV	R^2_{CV}	RPD_{CV}	SEP	R^2_P	Bias	Slope
Terpenoids														
α-Terpineol	2.5.5.1	153	0.35	0.74	7	0.12	0.97	0.18	0.94	4.11	0.50	0.80	0.11	1.05
Citral	2.5.5.1	143	14.54	7.99	4	4.05	0.74	5.42	0.56	1.47	52.11	0.02	21.22	−0.96
Linalool	1.5.5.1	151	1.69	2.00	10	0.43	0.95	0.69	0.88	2.90	4.10	0.20	1.24	0.73
p-Cymene	Snv-DT 1.5.5.1	144	0.19	0.32	4	0.094	0.91	0.13	0.89	2.46	1.62	0.26	0.62	1.87
Total terpenoids	Snv-DT 1.5.5.1	163	20.44	17.82	9	7.04	0.84	10.63	0.64	1.68	29.01	0.77	10.56	1.31
C_{13} norisoprenoids														
β-Damascenone	Snv-DT 1.5.5.1	157	0.19	0.56	10	0.11	0.96	0.17	0.90	3.29	0.92	0.70	0.30	1.52
β-Ionone	1.5.5.1	147	0.014	0.027	7	0.0061	0.95	0.0079	0.92	3.42	0.06	0.54	0.02	1.59
Total C_{13} norisoprenoids	2.5.5.1	145	0.050	0.20	8	0.039	0.96	0.074	0.92	2.70	1.53	0.18	0.66	1.91
Benzenoids														
Benzaldehyde	2.5.5.1	145	0.95	0.85	6	0.21	0.94	0.31	0.88	2.74	1.62	0.31	0.66	1.18
2-Phenylethanol	2.5.5.1	147	28.42	24.75	6	7.30	0.91	9.68	0.85	2.56	61.97	0.29	24.12	1.26
Benzyl alcohol	1.5.5.1	166	7.97	9.36	7	2.33	0.94	2.87	0.91	3.26	11.80	0.43	3.25	1.13
Total benzenoids	1.5.5.1	152	36.95	35.40	7	9.97	0.92	13.00	0.89	2.72	72.11	0.29	23.27	−0.62
Fatty acids														
Hexanoic acid	Snv-DT 1.5.5.1	140	3.64	3.29	5	1.38	0.82	1.85	0.70	1.78	18.28	0.006	5.02	0.47
Octanoic acid	1.5.5.1	152	1.03	0.84	8	0.25	0.91	0.34	0.83	2.47	1.60	0.17	0.41	0.71
Nonanoic acid	2.5.5.1	142	0.28	0.19	6	0.046	0.94	0.071	0.86	2.68	0.46	0.09	0.10	0.58
Decanoic acid	Snv-DT 2.5.5.1	128	0.082	0.039	2	0.021	0.70	0.023	0.65	1.70	0.12	0.12	0.03	1.16
Total fatty acids	1.5.5.1	159	21.38	17.99	7	8.54	0.77	10.74	0.64	1.68	27.76	0.19	3.45	0.73
C6 compounds														
2-Hexenal	1.5.5.1	145	131.30	80.33	4	22.89	0.92	28.77	0.87	2.79	364.85	0.006	145.27	0.37
Hexanal	1.5.5.1	156	230.19	167.62	8	28.48	0.97	36.75	0.95	4.56	429.60	0.30	111.34	1.45
1-Hexanol	Snv-DT 1.5.5.1	173	120.73	77.04	7	27.65	0.87	34.29	0.80	2.25	101.35	0.28	31.10	0.86
2-Hexen-1-ol	1.5.5.1	132	733.26	752.03	6	268.70	0.87	329.40	0.81	2.28	872.51	0.56	280.81	1.04
3-Hexen-1-ol	2.5.5.1	177	720.56	722.33	5	235.20	0.89	282.86	0.85	2.55	796.98	0.62	153.26	1.26
Total C6 compounds	Snv-DT 1.5.5.1	170	1914.64	1585.10	7	423.12	0.93	533.05	0.89	2.97	1805.04	0.53	509.87	1.08
Total positive compounds	Snv-DT 1.5.5.1	168	119.02	130.59	8	32.50	0.94	41.93	0.90	3.11	101.35	0.57	−9.77	0.69
TSS	Snv-DT 1.5.5.1	179	19.35	3.44	11	0.55	0.97	0.79	0.95	4.35	0.99	0.90	0.10	1.02

Note: Spectral treatment: four-figure code (*a.b.c.d*). where '*a*' refers to the number of the derivative, '*b*' is the gap over which the derivative is calculated, '*c*' corresponds to the number of data points in a running average or smoothing, and '*d*' refers to the second smoothing; Snv-DT, standard normal variate plus detrending; *N*, number of samples were the ones used for calibration and cross-validation models after chemical outlier detection ($t > 2.5$); SD, standard deviation; SEC, standard error of calibration; R^2_C, determination coefficient of calibration; SECV, standard error of cross-validation; R^2_{CV}, determination coefficient of cross-validation; RPD_{CV}, residual predictive deviation of cross-validation; SEP, standard error of prediction; R^2_P, determination coefficient of prediction. TSS, total soluble solids. Total positive compounds, the sum of all families except C6 compounds.

between 0.3 and 0.5 are considered to provide good separation between high and low values. The R^2_{CV} values between 0.5 and 0.7 provide good separation between high, medium and low values. The R^2_{CV} values between 0.7 and 0.9 are considered a good adjustment, and, finally, R^2_{CV} values ≥ 0.9 provide an excellent adjustment.[48] Table 2 shows that all the volatile compounds and their families had a $R^2_{CV} > 0.5$, so it can be affirmed that the models obtained for all the compounds and families can differentiate between high, medium, and low concentration values. In turn, all compounds and families except citral, total terpenoids, decanoic acid, and total fatty acids presented a $R^2_{CV} \geq 0.7$, which indicated that the concentration of these compounds can be quantified with the obtained models. This would have numerous benefits in the wine industry, allowing to classify grape berries according to their aromatic quality, as well as to choose the collected date accurately. The R^2 of a set of samples depends mainly on how those samples are distributed within the set. For this reason, the main difference between R^2_{CV} and R^2_P is the variability of the data from the calibration set, and from the prediction set, respectively. As the samples from the prediction set were randomly selected, and there were far fewer than those from the calibration set, they were not uniformly distributed over the entire range of concentrations, which is why R^2_P decreases, and there is such a difference with R^2_{CV}.

Table 2 also shows the number of LVs, a low number of LV favors the robustness and the generalization capability of the developed models, minimizing potential overfitting events, which ranged from 2 to 11, and the RPD_{CV}, which presented values from 1.47 to 4.56. RPD indicates the precision behavior of the prediction in comparison with the average of all the samples. Models with a RPD < 1.5 are not considered adequate, while those showing RPD values ranging from 1.5 to 2.0 are suitable for differentiating the variability of the data. However, RPD > 2 shows very good predictive performance, and RPD > 3 can be considered excellent.[51] It can be seen in Table 2 that all the models except for citral have a RPD > 1.5. In addition, the models obtained for the linalool, *p*-cymene, total C_{13} norisoprenoids, benzaldehyde, 2-phenylethanol, total benzenoids, octanoic acid, nonanoic acid, 2-hexenal, 1-hexanol, 2-hexen-1-ol, 3-hexen-1-ol, and total C6 compounds, have a $RPD_{CV} > 2$, thus showing very good predictive performance. Finally, the models obtained for the α-terpineol, β-damascenone, β-ionone, benzyl alcohol, hexanal, total positive compounds and TSS, show a $RPD_{CV} > 3$, so the predictive performance of these models can be considered excellent. Considering that volatile compounds are found in very low concentrations in grape berries, finding models that can predict their concentration throughout ripening by taking non-destructive spectral measurements, on intact berries, is a result of great value and with great applications in the future. For instance, to define the harvesting date accordingly to the aromatic profile of the aimed wine. That would be of special application in the production of sparkling *versus* still wines, in addition to considering the TSS and acidity parameters. However, some canopy management operations usually performed in the vineyard, such as defoliation, may have a direct impact on the metabolism (either biosynthesis or catabolism) of some aroma compounds.[66] Understanding the evolution of grape aroma composition along ripening may help to take informed decisions about the suitability or potential impact of carrying out a given canopy management operation.

The bias can be defined as the average difference between the spectroscopy-predicted value and the real one. A positive bias means that, on average, the model is over-estimating the composition of a specific compound by this amount whilst a negative value reflects underestimation.

Finally, the values of SEC, SECV, and SEP, which are the calibration, cross-validation, and prediction errors, respectively, can be observed in Table 2. The minimum values of SEC, SECV, and SEP were presented by β-ionone, being 0.0061 μg/L, 0.0079 μg/L, and 0.06 μg/L, respectively. The maximum values were presented by 2-hexen-1-ol, being 268.70 μg/L, 329.40 μg/L, and 872.51 μg/L, respectively. The removal of outliers reduced the range of concentrations covered by the models, leaving out of this range some samples of the prediction set (destined for external prediction). This caused a decrease in the prediction accuracy of samples outside this range, increasing the SEP.

In TSS, the PLS factor was 11, the RPD_{CV} was 4.35, the SEC was 0.55, the SECV was 0.79, and the SEP was 0.99. Furthermore, R^2_{CV} was > 0.9, so a non-invasive and non-contact model has been obtained that allows reliable, contactless quantification of °Brix throughout ripening.

Figure 3 shows the prediction models with a $R^2_P \geq 0.5$ in NIR range. In order to facilitate the interpretation of the results, the prediction samples (red color) are plotted next to the calibration model (black color). As it can be seen in Table 2, the number of samples used for the construction of the calibration models (four-fold cross-validation), which are represented in black, were: 153 for α-terpineol, 163 for total terpenoids, 157 for β-damascenone, 147 for β-ionone, 132 for 2-hexen-1-ol, 177 for 3-hexen-1-ol, 170 for total C6 compounds, and 168 for total positive compounds. The red samples correspond to the set of samples used for the external prediction (Table 1). Considering the large number of samples used to perform the calibration models (black color), Fig. 3 shows that, for the volatile compounds represented, most of the calibration samples are in the lower concentration range (as is normal for grape volatile compounds), with a very small number of samples in higher concentration ranges. This is the reason why the models yielded greater error values, when making the external prediction (red color), in the samples that were in the highest concentration ranges. This fact is well observed in Fig. 3(a),(c),(d)–(h) where the external prediction samples with highest concentrations are outside the prediction intervals (dashed lines).

However, for the TSS (Fig. 3(i)), it can be observed how the calibration samples (black) are well distributed throughout the entire °Brix range, so that when it comes to external prediction (red), little error is made, which decreases the SEP.

In addition, the loadings of the best PLS prediction models of volatile compounds and TSS, for the NIR spectral range: 1100–2100 nm, are plotted in Fig. 4. It can be seen how the wavelengths showing the highest loading weights of the latent variables are mainly located between 1100–1200 nm, 1300–1450 nm and 1850–1950 nm. This agrees with the absorption peaks found in the spectra.

As mentioned in the introduction, there are very few studies that have monitored the aromatic composition of grape berries by NIR spectroscopy.

In a work of Boido *et al.*[43] the volatile compounds of 97 samples of *Vitis vinifera* L. Tannat grape berries (red) were evaluated. The RPD_{CV} values obtained for volatile compounds in grape juice were > 2, except for two of the compounds. These RPD_{CV} values were much lower than those obtained in our work. However, in the work of Ripoll *et al.*[44] the profile of volatile compounds was studied in 52 samples of *Vitis vinifera* L. Albariño grapes (white) during three stages of maturation. A total of 26 volatile

Journal of The Science of Food and Agriculture published by John Wiley & Sons Ltd on behalf of Society of Chemical Industry.

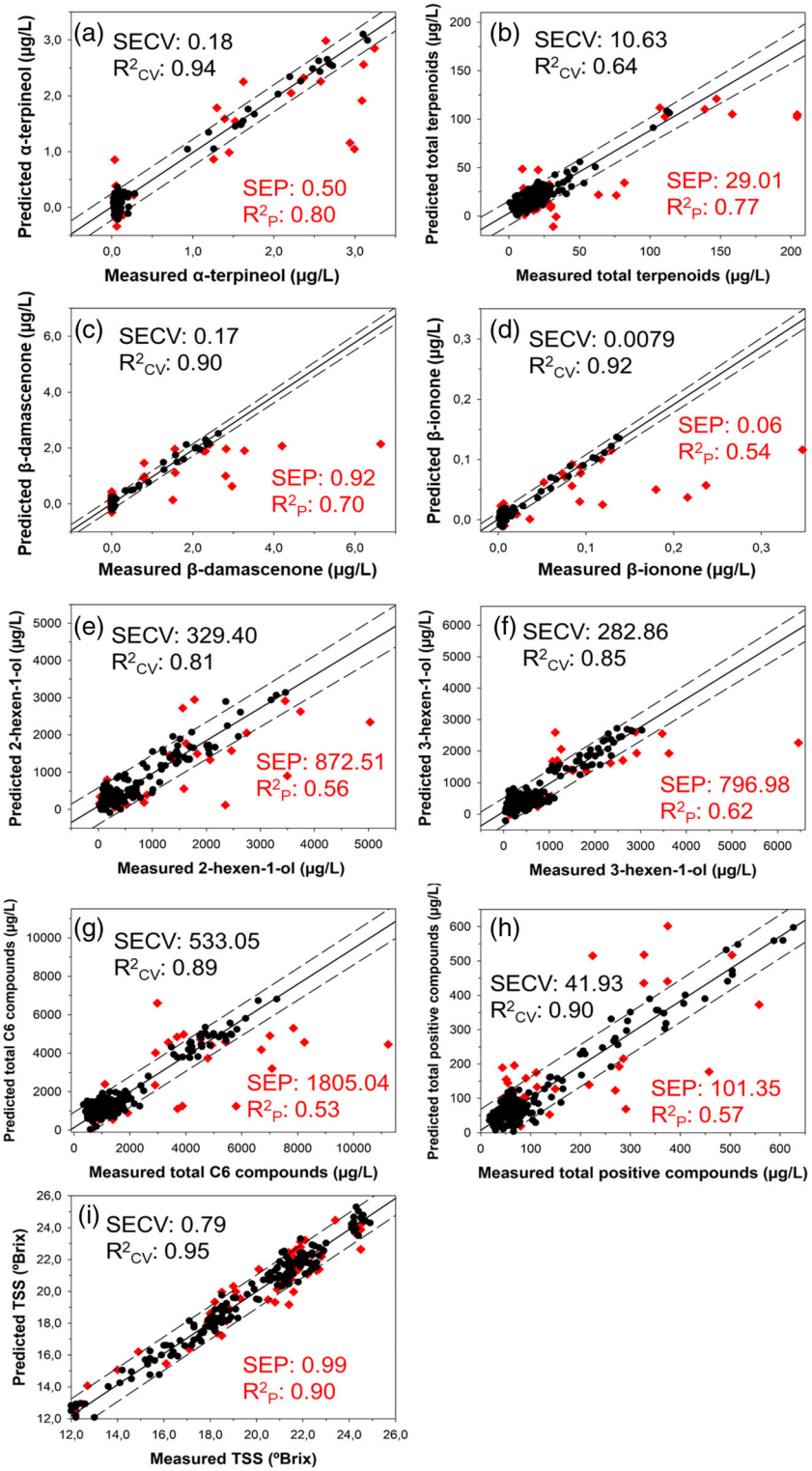

Figure 3. Regression plots for volatile compounds determination using the best PLS prediction models in the NIR range with $R^2_P > 0.5$: (a) α-terpineol; (b) total terpenoids; (c) β-damascenone; (d) β-ionone; (e) 2-hexen-1-ol; (f) 3-hexen-1-ol; (g) total C6 compounds; (h) total positive compounds (the sum of all families except C6 compounds); and (i) total soluble solids (TSS). Correlation line (solid) and predictions intervals (dashed lines).

compounds were identified, some of which are common to those studied in the present work. In the work of Ripoll *et al.*[44] the RPD_{CV} values ranged from 0.88 and 1.69, while. in the present study, in which 240 samples were analyzed, the RPD_{CV} was greater than 1.47 in all cases.

In a recent work of Gehlken *et al.*[45] volatile compounds were measured from a total of 725 grape mash samples, divided into more than 15 red and white grape varieties. The R^2_{CV} values obtained ranged from 0.251 to 0.926. Although the volatile compounds studied are different from those studied in our work,

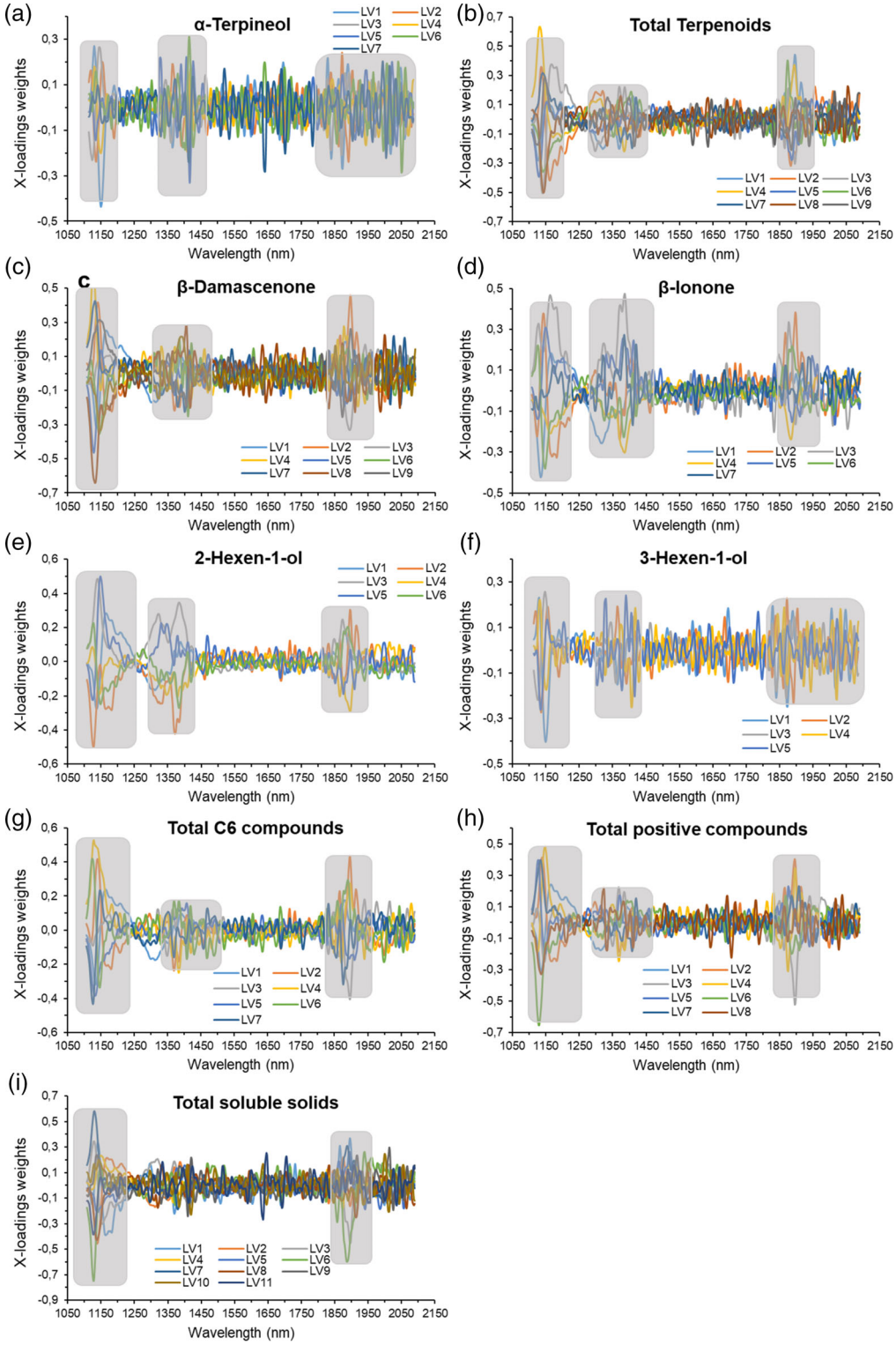

Figure 4. Loadings weight plots for all LVs of each volatile compounds and TSS determination using the best PLS prediction models in the NIR range. (a) α-terpineol; (b) total terpenoids; (d) β-ionone; (c) β-damascenone; (e) 2-hexen-1-ol; (f) 3-hexen-1-ol; (g) total C6 compounds; (h) total positive compounds; and (i) total soluble solids (TSS). Gray areas indicate the highest loading weights.

some of them such as linalool, hexanal, 2-hexenal, and 1-hexanol are common. In general, it can be observed that, in the aforementioned work, the R^2_{CV} and RPD_{CV} values are lower than those obtained in the present work. Focusing on the white varieties in particular, 25 of the 26 aromatic compounds identified in these varieties showed RPD_{CV} values less than 2, while most of the aromatic compounds identified in our work, showed RPD_{CV} values greater than 2, and even values greater than 3 in seven of them.

There are some works that evaluate TSS in grapes using NIR spectroscopy. In general, °Brix is a parameter that offers very good

Journal of The Science of Food and Agriculture published by John Wiley & Sons Ltd on behalf of Society of Chemical Industry.

results regardless of the NIR range, since sugars are found in very high concentrations in grapes. In the works found related to the grape varieties different to Tempranillo Blanco, the values of R^2_{CV}, R^2_P, and RPD_{CV} for the TSS are, respectively: 0.91, not calculated, and 3.34;[22] 0.93, not calculated, and 3.31;[67] 0.74, not calculated, and not calculated;[37] 0.90, 0.91, and 3.36;[30] and 0.95, 0.91, and 4.27.[12] However, to the best of our knowledge this is the first work applying NIR spectroscopy to estimate the aromatic composition and TSS in *Vitis vinifera* L. Tempranillo Blanco berries.

Based on the results obtained in the present work, the winegrower will be able to differentiate between high, medium, and low values of volatile compounds in *Vitis vinifera* L. Tempranillo Blanco grapes, as well as to quantify the TSS in a very reliable and accurate way, simultaneously. If the device is transported to the vineyard, it can track aromatic and technological maturity throughout the berry ripening period, as attempted by Fernández-Novales *et al*.[68] These authors estimated the TSS and the total amounts of anthocyanins and phenolics in Tempranillo berries from NIR spectroscopy acquired from a moving vehicle directly in the vineyard. This will enable estimating the harvest date more accurately according to oenological needs. In addition, if the device is installed in the winery, it could help to separate the grapes according to their aromatic quality, or their sugar content, creating fermentation tanks with different aromatic profiles, and finally obtaining wines with different characteristics and prices.

CONCLUSIONS

A new methodology, based on non-invasive, contactless NIR spectroscopy, has been developed to estimate volatile compounds content, as well as TSS, in *Vitis vinifera* L. Tempranillo Blanco intact grape berries throughout ripening. According to the results obtained, the obtained models would help to discriminate between high, medium, and low values in all volatile compounds, total content by chemical families, and TSS. In addition, the built models would enable to quantify the concentration of most volatile compounds, their chemical families, and the TSS content along ripening in *Vitis vinifera* L. Tempranillo Blanco berries.

For the first time, an easy, solvent-free, and fast tool has been developed that enables the estimation of technological and aromatic maturities simultaneously and non-invasively at different stages of ripening.

AUTHOR CONTRIBUTIONS

Sandra Marín-San Román: formal analysis, investigation, methodology, and writing – original draft. Juan Fernández-Novales: conceptualization, investigation, data curation, supervision, and writing – review and editing. Cristina Cebrián-Tarancón: data curation, methodology, and writing – review and editing. Rosario Sánchez-Gómez: data curation, methodology, and writing – review and editing. María Paz Diago: conceptualization, investigation, supervision, funding acquisition, and writing – review and editing. Teresa Garde-Cerdán: conceptualization, investigation, supervision, funding acquisition, and writing – review and editing.

ACKNOWLEDGEMENTS

Financial support was given by the Ministerio de Ciencia, Innovación y Universidades under the project RTI2018-096549-B-I00. Sandra Marín-San Román thanks Gobierno de La Rioja for her predoctoral contract.

CONFLICT OF INTEREST STATEMENT

The authors declare that they have no conflict of interest.

DATA AVAILABILITY STATEMENT

The data that support the findings of this study are available from the corresponding author upon reasonable request.

REFERENCES

1 Aleixandre-Tudo JL, Weightman C, Panzeri V, Nieuwoudt HH and Du TWJ, Effect of skin contact before and during alcoholic fermentation on the chemical and sensory profile of south African chenin blanc white wines. *South African J Enol Vitic* **36**:366–377 (2015).
2 Gambetta JM, Bastian SEP, Cozzolino D and Jeffery DW, Factors influencing the aroma composition of chardonnay wines. *J Agric Food Chem* **62**:6512–6534 (2014).
3 Marín-San Román S, Rubio-Bretón P, Pérez-Álvarez EP and Garde-Cerdán T, Advancement in analytical techniques for the extraction of grape and wine volatile compounds. *Food Res Int* **137**:1–13 (2020).
4 Castro-Mejías R, Natera-Marín R, Durán-Guerrero E and García-Barroso C, Application of solid phase extraction techniques to analyse volatile compounds in wines and other enological products. *Eur Food Res Technol* **228**:1–18 (2008).
5 López-Tamames E, Carro-Mariño N, Ziya Y, Sapis C, Baumes RL and Bayonove C, Potential aroma in several varieties of Spanish grapes. *J Agric Food Chem* **45**:1729–1735 (1997).
6 Martínez J, Rubio-Bretón P, Eva Vicente M and Enrique García-Escudero y, Influencia del terroir en el perfil aromático de Tempranillo Blanco en la D.O.Ca Rioja, in *E3S Web Conferences*, Vol. **50**, p. 2003 (2018). doi:10.1051/e3sconf/20185002003
7 Garde-Cerdán T, Rubio-Bretón P, Marín-San Román S, Baroja E, Sáenz de Urturi I and Pérez-Álvarez EP, Study of wine volatile composition of Tempranillo versus Tempranillo Blanco, a new white grape variety. *Beverages* **7**:1–12 (2021).
8 Ayestarán B, Martínez-Lapuente L, Guadalupe Z, Canals C, Adell E and Vilanova M, Effect of the winemaking process on the volatile composition and aromatic profile of Tempranillo Blanco wines. *Food Chem* **276**:187–194 (2019).
9 Garde-Cerdán T, da Costa NL, Rubio-Bretón P, Barbosa R, Baroja E, Martínez-Vidaurre JM *et al*., The Most important parameters to differentiate Tempranillo and Tempranillo Blanco grapes and wines through machine learning. *Food Anal Methods* **14**:2221–2236 (2021).
10 De CMBM, Del BVL, Gómez-Alonso S, García-Romero E and Hermosín I, Sensory descriptive and comprehensive GC–MS as suitable tools to characterize the effects of alternative winemaking procedures on wine aroma. Part I: BRS Carmem and BRS Violeta. *Food Chem* Elsevier **272**:462–470 (2019).
11 Kataoka H, Lord HL and Pawliszyn J, Applications of solid-phase microextraction in food analysis. *J Chromatogr A* Elsevier **880**:35–62 (2000).
12 Fernández-Novales J, Garde-Cerdán T, Tardáguila J, Gutiérrez-Gamboa G, Pérez-Álvarez EP and Diago MP, Assessment of amino acids and total soluble solids in intact grape berries using contactless Vis and NIR spectroscopy during ripening. *Talanta* Elsevier BV **199**:244–253 (2019).
13 Genisheva Z, Quintelas C, Mesquita DP, Ferreira EC, Oliveira JM and Amaral AL, New PLS analysis approach to wine volatile compounds characterization by near infrared spectroscopy (NIR). *Food Chem* Elsevier **246**:172–178 (2018).
14 Ramos MC and Martínez de Toda F, Variability in the potential effects of climate change on phenology and on grape composition of Tempranillo in three zones of the Rioja DOCa (Spain). *Eur J Agron* Elsevier **115**:126014 (2020).
15 Cataldo E, Fucile M and Mattii GB, Effects of kaolin and shading net on the ecophysiology and berry composition of sauvignon blanc grapevines. *Agriculture* **12**:1–21 (2022).
16 Martín-Verástegui B, *Influencia del cambio climático en el terroir y en los vinos de una zona de Ribera del Duero*. Univ. Valladolid. Esc. Técnica Super. Ing, Agrar (2019).
17 Benelli A, Cevoli C and Fabbri A, In-field Vis/NIR hyperspectral imaging to measure soluble solids content of wine grape berries during ripening, in *2020 IEEE International Workshop on Metrology for*

Agriculture and Forestry (MetroAgriFor), pp. 99–103 (2020). doi: 10.1109/MetroAgriFor50201.2020.9277621
18 Boido E, Fariña L, Carrau F, Cozzolino D and Dellacassa E, Application of near-infrared spectroscopy/artificial neural network to quantify glycosylated norisoprenoids in Tannat grapes. *Food Chem* **387**:132927 (2022).
19 Páscoa RNMJ, Porto PALS, Cerdeira AL and Lopes JA, The application of near infrared spectroscopy to wine analysis: an innovative approach using lyophilization to remove water bands interference. *Talanta* Elsevier B.V. **214**:120852 (2020).
20 Larraín M, Guesalaga AR and Agosin E, A multipurpose portable instrument for determining ripeness in wine grapes using NIR spectroscopy. *IEEE Trans Instrum Meas* **57**:294–302 (2008).
21 Herrera J, Guesalaga A and Agosin E, Shortwave-near infrared spectroscopy for non-destructive determination of maturity of wine grapes. *Meas Sci Technol* **14**:689–697 (2003).
22 González-Caballero V, Sánchez MT, López MI and Pérez-Marín D, First steps towards the development of a non-destructive technique for the quality control of wine grapes during on-vine ripening and on arrival at the winery. *J Food Eng* **101**:158–165 (2010).
23 Osborne BG, Fearn T and Hindle PT, *Practical NIR Spectroscopy: With Aplications in Food and Beverage Analysis*. Longman Scientific and Technical, London (1993).
24 Almeida PV, Rodrigues RP, Mendes CVT, Szeląg R, Pietrzyk D, Klepacz-Smółka A *et al*., Assessment of NIR spectroscopy for predicting biochemical methane potential of agro-residues – a biorefinery approach. *Biomass Bioenergy* **151**:106169 (2021).
25 McClure WF, 204 years of near infrared technology: 1800-2003. *J Near Infrared Spectrosc* **11**:487–518 (2003).
26 Barnaba FE, Bellincontro A and Mencarelli F, Portable NIR-AOTF spectroscopy combined with winery FTIR spectroscopy for an easy, rapid, in-field monitoring of Sangiovese grape quality. *J Sci Food Agric* **94**: 1071–1077 (2014).
27 Teixeira dos Santos CA, Páscoa RNMJ and Lopes JA, A review on the application of vibrational spectroscopy in the wine industry: From soil to bottle. *TrAC – Trends Anal Chem* **88**:100–118 (2017).
28 Marten GC, Shenk JS and Barton FE, Near infrared spectroscopy (NIRS): reflectance analysis of forage quality. *USDA Agric Handb* **643**:1–114 (1989).
29 Anjos O, Caldeira I, Roque R, Pedro SI, Lourenco S and Canas S, Screening of different ageing technologies of wine spirit by applications of near-infrared (NIR) spectroscopy and volatile quantification. *processes* **8**:1–18 (2020).
30 Urraca R, Sanz-Garcia A, Tardaguila J and Diago MP, Estimation of total soluble solids in grape berries using a hand-held NIR spectrometer under field conditions. *J Sci Food Agric* **96**:3007–3016 (2016).
31 Sleep B, Mason S, Janik L and Mosley L, Application of visible near-infrared absorbance spectroscopy for the determination of soil pH and liming requirements for broad-acre agriculture. *Precis Agric* Springer US **23**:194–218 (2022).
32 Ballesteros R, Intrigliolo DS, Ortega JF, Ramírez-Cuesta JM, Buesa I and Moreno MA, Vineyard yield estimation by combining remote sensing, computer vision and artificial neural network techniques. *Precis Agric* Springer US **21**:1242–1262 (2020).
33 Muganu M, Paolocci M, Gnisci D, Barnaba FE, Bellincontro A, Mencarelli F *et al*., Effect of different soil management practices on grapevine growth and on berry quality assessed by NIR-AOTF spectroscopy. *Acta Hortic* **978**:117–125 (2013).
34 Diezma-Iglesias B, Barreiro P, Blanco R and García-Ramos FJ, Comparison of robust modeling techniques on NIR spectra used to estimate grape quality. *Acta Hortic* **802**:367–372 (2008).
35 Martins RC, Barroso TG, Jorge P, Cunha M and Santos F, Unscrambling spectral interference and matrix effects in Vitis vinifera vis-NIR spectroscopy: towards analytical grade 'in vivo' sugars and acids quantification. *Comput Electron Agric* Elsevier B.V. **194**:106710 (2022).
36 Garde-Cerdán T, Lorenzo C, Zalacain A, Alonso GL and Salinas MR, Using near infrared spectroscopy to determine haloanisoles and halophenols in barrel aged red wines. *LWT – Food Sci Technol* Elsevier Ltd **46**:401–405 (2012).
37 Giovenzana V, Beghi R, Mena A, Civelli R, Guidetti R, Best S *et al*., Quick quality evaluation of Chilean grapes by a portable vis/NIR device. *Acta Hortic* **978**:93–100 (2013).
38 Cebrián-Tarancón C, Fernández-Roldán F, Alonso GL and Salinas RM, Classification of vine-shoots for use as enological additives. *J Sci Food Agric* **102**:724–731 (2022).
39 Garde-Cerdán T, Lorenzo C, L Alonso G and Salinas MR, Near infrared spectroscopy: easy and rapid tool to determine different volatile compounds in wines. *Curr Bioact Compd* **7**:93–105 (2011).
40 Lorenzo C, Garde-Cerdán T, Pedroza MA, Alonso GL and Salinas MR, Determination of fermentative volatile compounds in aged red wines by near infrared spectroscopy. *Food Res Int* Elsevier Ltd **42**: 1281–1286 (2009).
41 Garde-Cerdán T, Lorenzo C, Alonso GL and Rosario SM, Employment of near infrared spectroscopy to determine oak volatile compounds and ethylphenols in aged red wines. *Food Chem* Elsevier Ltd **119**: 823–828 (2010).
42 Smyth HE, Cozzolino D, Cynkar WU, Dambergs RG, Sefton M and Gishen M, Near infrared spectroscopy as a rapid tool to measure volatile aroma compounds in Riesling wine: possibilities and limits. *Anal Bioanal Chem* **390**:1911–1916 (2008).
43 Boido E, Fariña L, Carrau F, Dellacassa E and Cozzolino D, Characterization of glycosylated aroma compounds in Tannat grapes and feasibility of the near infrared spectroscopy application for their prediction. *Food Anal Methods* **6**:100–111 (2013).
44 Ripoll G, Vazquez M and Vilanova M, Ultraviolet – visible – near infrared spectroscopy for rapid determination of volatile compounds in white grapes during ripening. *Cienc e Tec Vitivinic* **32**:53–61 (2017).
45 Gehlken J, Pour Nikfardjam M and Zörb C, Determination of aroma compounds in grape mash under conditions of tasting by on-line near-infrared spectroscopy. *Eur Food Res Technol* Springer Berlin Heidelberg **248**:2325–2337 (2022).
46 Marín-San Román S, Carot-Sierra JM, Sáenz de Urturi I, Rubio-Bretón P, Pérez-Álvarez EP and Garde-Cerdán T, Optimization of thin film-microextraction (TF-SPME) method in order to determine musts volatile compounds. *Anal Chim Acta* Elsevier BV **1226**:1–12 (2022).
47 Sánchez-Gómez R, Zalacain A, Alonso GL and Salinas MR, Vine-shoot waste aqueous extracts for re-use in agriculture obtained by different extraction techniques: phenolic, volatile, and mineral compounds. *J Agric Food Chem* **62**:10861–10872 (2014).
48 Shenk JS and Westerhaus MO, Routine operation, calibration, development and network system management manual. *NIRSystems Inc, Silver Spring* **3** (1995).
49 Massart DL, Vandeginste EGM, Deming SN, Michotte Y, Kaufman L and Bertsch W, Chemometrics: ATextbook (1988).
50 Næs T, Isaksson T, Fearn T and Davies T, A user-friendly guide to Multivariate Calibration and Classification (2017).
51 Williams PC and Sobering DC, How do we do it: a brief summary of the methods we use in developing near infrared calibration. *Near Infrared Spectroscopy: The Future Waves*:185–188 (1996).
52 Martin MA and Roberts S, An evaluation of bootstrap methods for outlier detection in least squares regression. *J Appl Stat* **33**:703–720 (2006).
53 Rubio-Bretón P, Salinas MR, Nevares I, Pérez-Álvarez EP, del Álamo-Sanza M, Marín-San Román S *et al*., Recent advances in the study of grape and wine volatile composition: varietal, fermentative, and aging aroma compounds, in *Food Aroma Evolution During Food Processing, Cooking, and Aging*, 1st editio edn, ed. by Bordiga M and Nollet LML. CRC Press, Boca Raton, FL, USA, pp. 439–463 (2019).
54 Darriet P, Thibon C and Dubourdieu D, Aroma and aroma precursors in grape berry. *Biochemistry Grape Berry*:111–136 (2012). doi: 10.2174/978160805360511201010111
55 González-Barreiro C, Rial-Otero R, Cancho-Grande B and Simal-Gándara J, Wine aroma compounds in grapes: a critical review. *Crit Rev Food Sci Nutr* **55**:202–218 (2015).
56 Black CA, Parker M, Siebert TE, Capone DL and Francis IL, Terpenoids and their role in wine flavour: recent advances. *Aust J Grape Wine Res* **21**:582–600 (2015).
57 Mendes-Pinto MM, Carotenoid breakdown products the-norisoprenoids-in wine aroma. *Arch Biochem Biophys* Elsevier Inc **483**:236–245 (2009).
58 Styger G, Prior B and Bauer FF, Wine flavor and aroma. *J Ind Microbiol Biotechnol* **38**:1145–1159 (2011).
59 Gutiérrez-Gamboa G, Garde-Cerdán T, Rubio-Bretón P and Pérez-Álvarez EP, Seaweed foliar applications at two dosages to Tempranillo Blanco (Vitis vinifera L.) grapevines in two seasons: effects on grape and wine volatile composition. *Food Res Int* Elsevier Ltd **130**: 108918 (2020).
60 Robinson AL, Boss PK, Solomon PS, Trengove RD, Heymann H and Ebeler SE, Origins of grape and wine flavor. Part 1. Chemical components and viticultural impacts. *Am J Enol Vitic* **1**:1–24 (2014).

61 Garde-Cerdán T, Santamaría P, Rubio-Bretón P, González-Arenzana L, López-Alfaro I and López R, Foliar application of proline, phenylalanine, and urea to Tempranillo vines: effect on grape volatile composition and comparison with the use of commercial nitrogen fertilizers. *LWT – Food Sci Technol* **60**:684–689 (2015).
62 García E, Chacón JL, Martínez J and Izquierdo PM, Changes in volatile compounds during ripening in grapes of Airén, Macabeo and chardonnay white varieties grown in La Mancha region (Spain). *Food Sci Technol Int* **9**:33–41 (2003).
63 Marín-San Román S, Garde-Cerdán T, Baroja E, Rubio-Bretón P and Pérez-Álvarez EP, Foliar application of phenylalanine plus methyl jasmonate as a tool to improve grenache grape aromatic composition. *Sci Hortic (Amsterdam)* Elsevier **272**:109515 (2020).
64 Alem H, Rigou P, Schneider R, Ojeda H and Torregrosa L, Impact of agronomic practices on grape aroma composition: a review. *J Sci Food Agric* **99**:975–985 (2018).
65 D'Onofrio C, Matarese F and Cuzzola A, Effect of methyl jasmonate on the aroma of Sangiovese grapes and wines. *Food Chem* Elsevier **242**: 352–361 (2018).
66 Cataldo E, Salvi L, Paoli F, Fucile M and Mattii GB, Effect of agronomic techniques on aroma composition of white grapevines: a review. *Agronomy* **11**:1–19 (2021).
67 Bellincontro A, Cozzolino D and Mencarelli F, Application of NIR-AOTF spectroscopy to monitor Aleatico grape dehydration for Passito wine production. *Am J Enol Vitic* **62**:256–260 (2011).
68 Fernández-Novales J, Tardáguila J, Gutiérrez S and Diago MP, On-the-go VIS + SW – NIR spectroscopy as a reliable monitoring tool for grape composition within the vineyard. *Molecules* **24**:1–15 (2019).

Journal of The Science of Food and Agriculture published by John Wiley & Sons Ltd on behalf of Society of Chemical Industry.